JOC Article

Theoretical Study on the Mechanism of the [2 + 1] Thermal Cycloaddition between Alkenes and Stable Singlet (Phosphino)(silyl)carbenes†

Begoña Lecea,‡ Mirari Ayerbe,‡ Ana Arrieta,§ Fernando P. Cossío,*,§ Vicenç Branchadell,*,|| Rosa M. Ortuño,|| and Antoine Baceiredo⊥

Farmazi Fakultatea, Kimika Organikoa I Saila, Universidad del País Vasco−Euskal Herriko Unibertsitatea, P. K. 450, 01080 Vitoria-Gasteiz, Spain, Kimika Fakultatea, Kimika Organikoa I Saila, Universidad del País Vasco−Euskal Herriko Unibertsitaea, P. K. 1071, 28080 San Sebastián-Donostia, Spain, Departament de Química, Universitat Autònoma de Barcelona, 08193 Bellaterra, Barcelona, Spain, and Laboratoire Hétérochimie Fondamentale et Appliquée, UMR 5069, Université Paul Sabatier, 118 Route de Narbonne, 31062 Toulouse Cedex 9, France

fp.cossio@ehu.es; vicenc.branchadell@uab.es

Received August 10, 2006

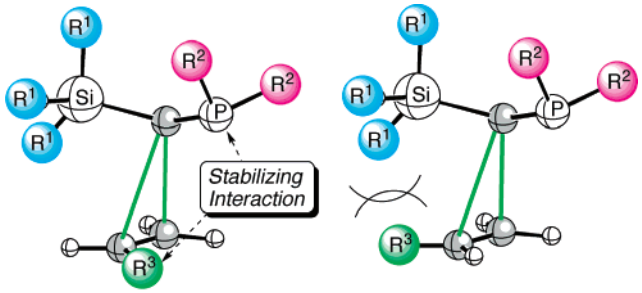

The mechanism and the origins of the stereocontrol observed in the reaction between differently substituted alkenes and stable (phosphino)(silyl)carbenes giving cyclopropanes have been studied computationally. These cyclopropanation reactions proceed via asynchronous concerted mechanisms involving early transition structures with a significant charge transfer from the carbene to the alkene moiety. The geometric features of these transition structures preclude a significant overlap between the orbitals required for secondary orbital interactions between the reactants. The stereoselectivity observed experimentally stems from favorable electrostatic and steric interactions between the reactants leading to the stereoisomers in which the phosphanyl and carbonyl or aryl groups are cis to each other.

Introduction

The [2 + 1] thermal cycloaddition between carbenes and alkenes is a general and useful method for the convergent synthesis of cyclopropane rings (Scheme 1).[1] Several approaches have been developed to carry out this important reaction, many of them relying on the use of transition metals to generate the reactive species or to catalyze the reaction.[2] However, since the discovery of stable singlet carbenes,[3,4] the study of the reactivity of these species and in particular their [2 + 1] cycloadditions with alkenes has received renewed interest. Thus, the reactivity of (phosphino)(silyl)carbenes with mono- and

† Dedicated to Prof. Marcial Moreno-Mañas in memoriam.

* Corresponding author. Phone: 34-943-015442; fax: 34-943-015270.
‡ Farmazi Fakultatea, Universidad del País Vasco−Euskal Herriko Unibertsitatea.
§ Kimika Fakultatea, Universidad del País Vasco−Euskal Herriko Unibertsitatea.
|| Universitat Autònoma de Barcelona.
⊥ Université Paul Sabatier.

(1) (a) Moss, R. *Acc. Chem. Rev.* **1989**, *22*, 15. (b) Lebel, H.; Marcoux, J.-P.; Molinaro, C.; Charette, A. B. *Chem. Rev.* **2003**, *103*, 977. (c) Helquist, P. In *Comprehensive Organic Synthesis*; Trost, B. M., Fleming, I., Semmelhack, M. F., Eds.; Pergamon: Oxford, 1991; Vol. 4, pp 951−997.

(2) (a) Doyle, M. P. *Chem. Rev.* **1986**, *86*, 919. (b) Lautens, M.; Klute, W.; Tam, W. *Chem. Rev.* **1996**, *96*, 49.

(3) (a) Bourissou, D.; Guerret, O.; Gabbaï, F. P.; Bertrand, G. *Chem. Rev.* **2000**, *100*, 39. (b) Herrmann, W. A.; Köcher, C. *Angew. Chem., Int. Ed. Engl.* **1997**, *36*, 2162. (c) Arduengo, A. J., III. *Acc. Chem. Res.* **1999**, *32*, 913.

10.1021/jo061662v CCC: $37.00
Published on Web 12/13/2006

SCHEME 1. General [2 + 1] Cycloaddition between Singlet Carbenes and Alkenes To Form Cyclopropanes[a]

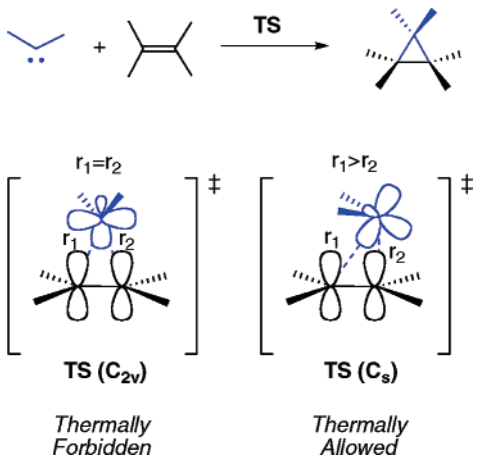

[a] The possible substituents at the different positions are not specified. The two alternative geometries for the transition state are also given, assuming a CX_2−ethylene interaction.

trans-disubstituted alkenes has been reported to proceed with high chemical yields and with complete diastereoselectivity in favor of the corresponding *cis*-cyclopropanes, in which the phosphino group and the substituent of the alkene are in a cis-relationship to each other.[5,6] This methodology has been extended to the efficient synthesis of enantiopure cyclopropanes by using either alkenes[7] or carbenes themselves[8] as the source of chirality.

Aside from the practical importance of this reaction, its mechanistic study is also very interesting from a theoretical−computational standpoint since it constitutes the simplest case of a thermal cycloaddition.[9] It is interesting to note that the non-intuitive mechanism usually accepted for this reaction was proposed in 1956 and 1958 on the basis of experimental observations.[10] Almost one decade later, Hoffmann published the first rationalization of this proposal on the basis of theoretical considerations.[11] According to this model, the [2 + 1] cycloaddition involves the electrophilic approach of the carbene vacant p AO to the π orbital of the olefin and the interaction of the carbene filled sp^2-hybridized AO with the π^* orbital of the alkene. In this way, the reactants avoid the forbidden least motion approach within the C_{2v} symmetry point group for the CX_2−ethylene system (Scheme 1).

Since this seminal work, other authors have explored computationally this reaction. Thus, SCF−MO calculations on singlet carbenes such as CF_2, CCl_2, CFOH, and $C(OH)_2$ showed concerted although asynchronous mechanisms compatible with the C_s symmetric mechanism shown in Scheme 1.[12,13] These calculations allowed us to associate the ratio between the so-called electrophilic and nucleophilic bond-forming distances (r_1 and r_2 values in Scheme 1, respectively) with the electrophilic or nucleophilic character of the corresponding singlet carbenes. On the other hand, MCSCF/MP2 calculations[14] suggested that the cyclopropanation reaction involving unsubstituted alkenes can be an asynchronous but concerted processes, whereas those reactions involving simple carbenes and bulky substituted alkenes are likely to take place via stepwise mechanisms involving singlet diradicals. Finally, DFT calculations[15] at the B3LYP/6-31G* level on several singlet carbenes and alkenes such as ethylene, cyanoethylene, *trans*-2-butene, and dimethyl-2-butene showed that there is a complex electronic flow between both reactants, although there is a predominant electron transfer from the alkene to the carbene carbon. It is noteworthy that, to the best of our knowledge, there is no previous report on the stereoselectivity of these [2 + 1] thermal cycloadditions.

Within this context, the aim of the present work has been to investigate computationally the main features of [2 + 1] cycloadditions between alkenes and several singlet (phosphino)-(silyl)carbenes. In addition, we have investigated the origins of the experimentally observed complete *cis*-sterocontrol in the thermal [2 + 1] cycloaddition between these stabilized carbenes and mono- and disubstituted alkenes.[5−8] The carbenes and the cyclopropanation reactions studied are reported in Scheme 2.

(4) For selected examples of fully characterized phosphorous and/or silicon containing singlet carbenes, see: (a) Martin, D.; Baceiredo, A.; Gornitzka, H.; Schoeller, W. W.; Bertrand, G. *Angew. Chem., Int. Ed.* **2005**, *44*, 1700. (b) Merceron-Saffon, N.; Baceiredo, A.; Gornitzka, H.; Bertrand, G. *Science* **2003**, *301*, 123. (c) Solé, S.; Gornitzka, H.; Schoeller, W. W.; Bourissou, D.; Bertrand, G. *Science* **2001**, *292*, 1901. (d) Kato, T.; Gornitzka, H.; Baceiredo, A.; Savin, A.; Bertrand, G. *J. Am. Chem. Soc.* **2000**, *122*, 998.

(5) (a) Igau, A.; Grützmacher, H.; Baceiredo, A.; Bertrand, G. *J. Am. Chem. Soc.* **1988**, *110*, 6463. (b) Igau, A.; Baceiredo, A.; Trinquier, G.; Bertrand, G. *Angew. Chem., Int. Ed. Engl.* **1989**, *28*, 621.

(6) Gourmi-Magnet, S.; Kato, T.; Gornitzka, H.; Baceiredo, A.; Bertrand, G. *J. Am. Chem. Soc.* **2000**, *122*, 4464.

(7) Krysiak, J.; Kato, T.; Gornitzka, H.; Baceiredo, A.; Mikolajczyk, M.; Bertrand, G. *J. Org. Chem.* **2001**, *66*, 8240.

(8) Krysiak, J.; Lyon, C.; Baceiredo, A.; Gornitzka, H.; Mikolajczyk, M.; Bertrand, G. *Chem.—Eur. J.* **2004**, *10*, 1982.

(9) Krogh-Jespersen, K.; Yan, S.; Moss, R. *J. Am. Chem. Soc.* **1999**, *121*, 6269.

(10) (a) Skell, P. S.; Garner, A. Y. *J. Am. Chem. Soc.* **1956**, *78*, 5430. (b) von Doering, W. E.; Henderson, W. A., Jr. *J. Am. Chem. Soc.* **1958**, *80*, 5274. See also: (c) Skell, P. S.; Cholod, M. S. *J. Am. Chem. Soc.* **1969**, *91*, 7131.

(11) (a) Hoffmann, R. *J. Am. Chem. Soc.* **1968**, *90*, 1475. (b) Hoffmann, R.; Hayes, D. M.; Skell, P. S. *J. Phys. Chem.* **1972**, *76*, 664.

(12) (a) Rondan, N. G.; Houk, K. N.; Moss, R. A. *J. Am. Chem. Soc.* **1980**, *102*, 1770. (b) Houk, K. N.; Rondan, N. G.; Mareda, J. *J. Am. Chem. Soc.* **1984**, *106*, 4291. (c) Houk, K. N.; Rondan, N. L.; Mareda, J. *Tetrahedron* **1985**, *41*, 1555. (d) Evanseck, J. D.; Mareda, J.; Houk, K. N. *J. Am. Chem. Soc.* **1990**, *112*, 73.

(13) Blake, J. F.; Wierschke, S. G.; Jorgensen, W. L. *J. Am. Chem. Soc.* **1989**, *111*, 1919.

(14) Bernardi, F.; Bottoni, A.; Canepa, C.; Olivucci, M.; Robb, M. A.; Tonachini, G. *J. Org. Chem.* **1997**, *62*, 2018.

(15) Mendez, F.; Garcia-Garibay, M. A. *J. Org. Chem.* **1999**, *64*, 7061.

(16) Parr, R. G.; Yang, W. *Density Functional Theory of Atoms and Molecules*; Oxford: New York, 1989.

(17) (a) Kohn, W.; Becke, A. D.; Parr, R. G. *J. Phys. Chem.* **1996**, *100*, 12974. (b) Becke, A. D. *J. Chem. Soc.* **1993**, *98*, 5648. (c) Becke, A. D. *Phys. Rev. A* **1988**, *38*, 3098. (d) Lee, C.; Yang, W.; Parr, R. G. *Phys. Rev. B* **1998**, *37*, 785. (e) Vosko, S. H.; Wilk, L.; Nusair, M. *Can. J. Phys.* **1980**, *58*, 1200.

(18) Hehre, W. J.; Radom, L.; Schleyer, P. v. R.; Pople, J. A. *Ab Initio Molecular Orbital Theory*; Wiley: New York, 1986; pp 76−87 and references therein.

(19) Frisch, M. J.; Trucks, G. W.; Schlegel, H. B.; Scuseria, G. E.; Robb, M. A.; Cheeseman, J. R.; Zakrzewski, V. G.; Montgomery, J. A., Jr.; Stratmann, R. E.; Burant, J. C.; Dapprich, S.; Millam, J. M.; Daniels, A. D.; Kudin, K. N.; Strain, M. C.; Farkas, O.; Tomasi, J.; Barone, V.; Cossi, M.; Cammi, R.; Mennucci, B.; Pomelli, C.; Adamo, C.; Clifford, S.; Ochterski, J.; Petersson, G. A.; Ayala, P. Y.; Cui, Q.; Morokuma, K.; Malick, D. K.; Rabuck, A. D.; Raghavachari, K.; Foresman, J. B.; Cioslowski, J.; Ortiz, J. V.; Stefanov, B. B.; Liu, G.; Liashenko, A.; Piskorz, P.; Komaromi, I.; Gomperts, R.; Martin, R. L.; Fox, D. J.; Keith, T.; Al-Laham, M. A.; Peng, C. Y.; Nanayakkara, A.; Gonzalez, C.; Challacombe, M.; Gill, P. M. W.; Johnson, B.; Chen, W.; Wong, M. W.; Andres, J. L.; Gonzalez, C.; Head-Gordon, M.; Replogle, E. S.; Pople, J. A. *Gaussian 98*, revision A; Gaussian, Inc.: Pittsburgh PA, 1998.

SCHEME 2. Reactions between Singlet (Phosphino)(silyl)carbenes and Mono- and Disubstituted Olefins Presented in This Study[a]

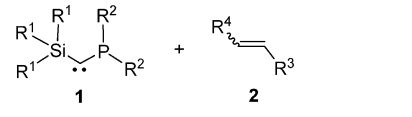

1 **2**

1a: $R^1=R^2=H$ **2a**: $R^3=R^4=H$
1b: $R^1=H$; $R^2=NH_2$ **2b**: $R^3=COOMe$; $R^4=H$
1c: $R^1=H$; $R^2=NMe_2$ **2c**: $R^3=CONMe_2$; $R^4=H$
1d: $R^1=Me$; $R^2=NMe_2$ **2d**: $R^3=Ph$; $R^4=H$
1e: $R^1=Me$; $R^2=N^iPr_2$ **2e**: $R^3=R^4=COOMe$ (*E*)
2f : $R^3=R^4=COOMe$ (*Z*)

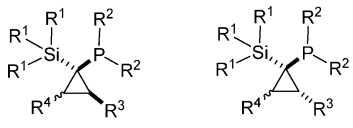

***cis*-3** ***trans*-3**

3aa: $R^1=R^2=R^3=R^4=H$
3ba: $R^1=R^3=R^4=H$; $R^2=NH_2$
3bb: $R^1=R^4=H$; $R^2=NH_2$; $R^3=COOMe$
3ca: $R^1=R^3=R^4=H$; $R^3=COOMe$
3cb: $R^1=R^4=H$; $R^2=NMe_2$; $R^3=COOMe$
3cc: $R^1=R^4=H$; $R^2=NMe_2$; $R^3=CONMe_2$
3ce: $R^1=H$; $R^2=NMe_2$; $R^3=R^4=COOMe$ (*E*)
3cf : $R^1=H$; $R^2=NMe_2$; $R^3=R^4=COOMe$ (*Z*)
3ee: $R^1=Me$; $R^2=N^iPr_2$; $R^3=R^4=COOMe$ (*E*)
3ef : $R^1=Me$; $R^2=N^iPr_2$; $R^3=R^4=COOMe$ (*Z*)
3db: $R^1=Me$; $R^2=NMe_2$; $R^3=COOMe$; $R^4=H$
3dc: $R^1=Me$; $R^2=NMe_2$; $R^3=CONMe_2$; $R^4=H$
3dd: $R^1=Me$; $R^2=NMe_2$; $R^3=Ph$; $R^4=H$
3ec: $R^1=Me$; $R^2=N^iPr_2$; $R^3=CONMe_2$; $R^4=H$

[a] Cis- and trans-descriptors correspond to the relative stereochemistry between the PR^2_2 and R^3 groups.

Computational Methods

All the calculations reported in this paper have been performed within the Density Functional Theory,[16] using the hybrid three-parameter functional customarily denoted as B3LYP.[17] The standard 6-31G* basis set[18] as implemented in the *GAUSSIAN 98*[19] and *GAUSSIAN 03*[20] suites of programs has been used in all cases.[21]

The synchronicity[22] of the reactions was calculated by using a previously described approach.[23] For a given concerted reaction,

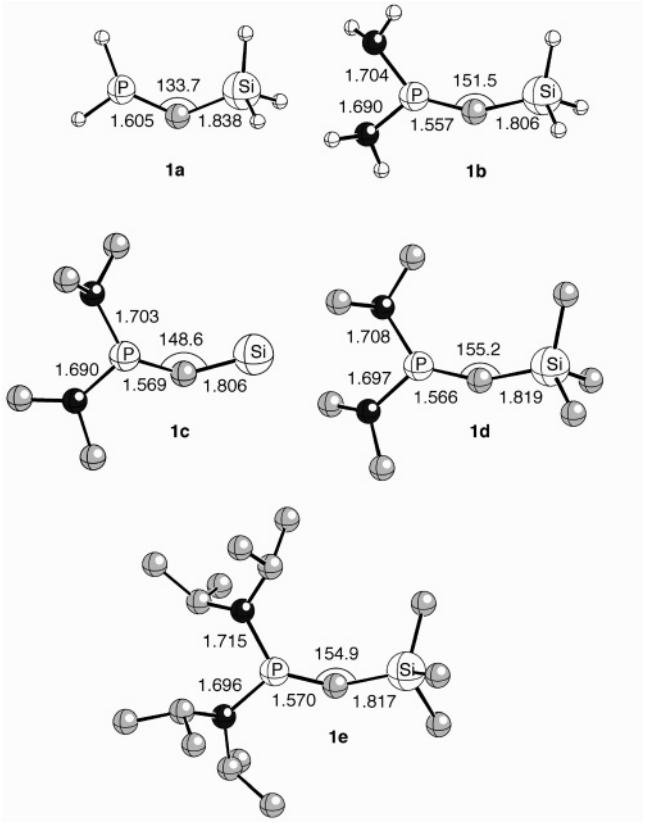

FIGURE 1. Fully optimized structures (B3LYP/6-31G* level) of (phosphino)(silyl)carbenes **1a**−**e**. Bond distances and angles are given in angstroms and degrees, respectively. Unless otherwise stated, white, gray, and blue denote hydrogen, carbon, and nitrogen atoms, respectively. Hydrogen atoms in compounds **1c**−**e** are not shown for clarity.

synchronicity (*Sy*) is quantified as

$$Sy = 1 - (2n-2)^{-1}\sum_{i=1}^{n}\frac{|\delta B_i - \delta B_{av}|}{\delta B_{av}} \qquad (1)$$

where n is the number of bonds directly involved in the reaction and δB_i is the relative variation of the bond index B_i at the transition structure (TS) relative to the reactant(s) (R) and product (P), according to the following expression:

$$\delta B_i = \frac{B_i^{TS} - B_i^{R}}{B_i^{P} - B_i^{R}} \qquad (2)$$

The average value of δB_i, denoted as δB_{av} in eq 1, therefore is

$$\delta B_{av} = n^{-1}\sum_{i=1}^{n}\delta B_i \qquad (3)$$

Wiberg indices B_i were employed;[24] these were evaluated using

(20) Frisch, M. J.; Trucks, G. W.; Schlegel, H. B.; Scuseria, G. E.; Robb, M. A.; Cheeseman, J. R.; Montgomery, J. A., Jr.; Vreven, T.; Kudin, K. N.; Burant, J. C.; Millam, J. M.; Iyengar, S. S.; Tomasi, J.; Barone, V.; Mennucci, B.; Cossi, M.; Scalmani, G.; Rega, N.; Petersson, G. A.; Nakatsuji, H.; Hada, M.; Ehara, M.; Toyota, K.; Fukuda, R.; Hasegawa, J.; Ishida, M.; Nakajima, T.; Honda, Y.; Kitao, O.; Nakai, H.; Klene, M.; Li, X.; Knox, J. E.; Hratchian, H. P.; Cross, J. B.; Bakken, V.; Adamo, C.; Jaramillo, J.; Gomperts, R.; Stratmann, R. E.; Yazyev, O.; Austin, A. J.; Cammi, R.; Pomelli, C.; Ochterski, J. W.; Ayala, P. Y.; Morokuma, K.; Voth, G. A.; Salvador, P.; Dannenberg, J. J.; Zakrzewski, V. G.; Dapprich, S.; Daniels, A. D.; Strain, M. C.; Farkas, O.; Malick, D. K.; Rabuck, A. D.; Raghavachari, K.; Foresman, J. B.; Ortiz, J. V.; Cui, Q.; Baboul, A. G.; Clifford, S.; Cioslowski, J.; Stefanov, B. B.; Liu, G.; Liashenko, A.; Piskorz, P.; Komaromi, I.; Martin, R. L.; Fox, D. J.; Keith, T.; Al-Laham, M. A.; Peng, C. Y.; Nanayakkara, A.; Challacombe, M.; Gill, P. M. W.; Johnson, B.; Chen, W.; Wong, M. W.; Gonzalez, C.; Pople, J. A. *Gaussian 03*, revision C.02; Gaussian, Inc.: Wallingford, CT, 2004.

(21) Although the B3LYP/6-31.G* level is not free from limitations, it constitutes a convenient method for the computational treatment of pericyclic reactions. See, for example: (a) Guner, V.; Khuong, K. S.; Leach, A. G.; Lee, P. S.; Bartberger, M. D.; Houk, K. N. *J. Phys. Chem. A* **2003**, *107*, 11445. (b) Goumans, T. P. M.; Ehler, A. W.; Lammertsma, K.; Würthwein, E.-V.; Grimme, S. *Chem.—Eur. J.* **2004**, *10*, 6468.

(22) (a) Borden, W. T.; Loncharich, R. J.; Houk, K. N. *Annu. Rev. Phys. Chem.* **1988**, *39*, 213. (b) Moyano, A.; Pericàs, M. A.; Valentí, E. *J. Org. Chem.* **1989**, *54*, 573.

(23) (a) Cossío, F. P.; Morao, I.; Jiao, H.; Schleyer, P. v. R. *J. Am. Chem. Soc.* **1999**, *121*, 6737. (b) Morao, I.; Lecea, B.; Cossío, F. P. *J. Org. Chem.* **1997**, *62*, 7033. (c) Lecea, B.; Arrieta, A.; Roa, G.; Ugalde, J. M.; Cossío, F. P. *J. Am. Chem. Soc.* **1994**, *116*, 9613. (d) Lecea, B.; Arrieta, A.; Lopez, X.; Ugalde, J. M.; Cossío, F. P. *J. Am. Chem. Soc.* **1995**, *117*, 12314.

(24) Wiberg, K. B. *Tetrahedron* **1968**, *24*, 1083.

TABLE 1. Calculated[a] Atomic Charges of the Carbene Moiety ($q_{(C:)}$, in au), :C−Si and :C−P Bond Orders (B(:C−Si) and B(:C−P), Respectively), Hardenesses[b] (η, in au), Chemical Potentials[c] (μ, in au), Global Electrophilicities[d] (ω, in eV), and Maximum Number of Accepted Electrons[e] (ΔN_{max}, in au) of (Phosphino)(silyl)carbenes 1a−e and Singlet Carbenes CH_2 and CCl_2

carbene	$q_{(C:)}$	B(:C−Si)	B(:C−P)	η	μ	ω	ΔN_{max}
1a	−1.032	0.903	2.097	0.15074	−0.14722	1.94	0.977
1b	−1.337	0.888	2.166	0.18982	−0.10637	0.80	0.560
1c	−1.310	0.898	2.130	0.17539	−0.10281	0.82	0.586
1d	−1.344	0.812	2.151	0.17322	−0.09450	0.70	0.546
1e	−1.357	0.819	2.108	0.16434	−0.09045	0.67	0.550
:CH_2 (C_{2v})	−0.170			0,12198	−0.18242	3.68	1.495
:CCl_2 (C_{2v})	−0.087			0.13986	−0.20044	3.88	1.433

[a] Computed at the B3LYP/6-31G* level. [b] Computed according to eq 5. [c] Computed according to eq 6. [d] Computed according to eq 7. [e] Computed according to eq 8.

SCHEME 3. Extreme Model Transition Structures for the Cyclopropanation Reaction Involving Electrophilic (A) and Nucleophilic (B) Carbenes

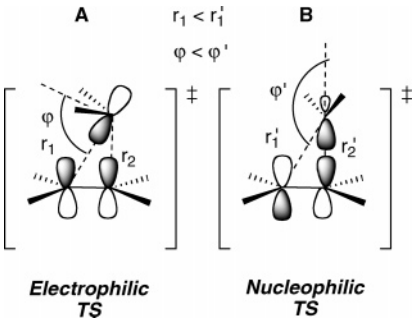

TABLE 2. Activation Energies[a] (ΔE_a, kcal/mol), Reaction Energies[a] (ΔE_{rxn}, kcal/mol), Natural Charges of the Carbene Moiety at the Corresponding Transition Structures (Σq(1), in au), Degrees of Advancement of the Transition Structures[b] (δB_{av}), and Synchronicities[c] (Sy) for Several Reactions Depicted in Scheme 2

reactants	TS	product	ΔE_a	ΔE_{rxn}	$\sum$q(1)	δB_{av}	Sy
1a + 2a	**TSaa**	**3aa**	9.4	−65.0	−0.100	0.203	0.91
1b + 2a	**TSba**	**3ba**	20.0	−56.2	−0.098	0.217	0.90
1c + 2a	**TSca**	**3ca**	11.4	−52.8	−0.091	0.248	0.82
1c + 2b	***cis*-TScb**	***cis*-3cb**	5.5	−49.8	0.105	0.262	0.68
1c + 2b	***trans*-TScb**	***trans*-3cb**	8.6	−48.6	0.058	0.244	0.73
1d + 2b	***cis*-TSdb**	***cis*-3db**	6.7	−42.7	0.153	0.271	0.66
1d + 2b	***trans*-TSdb**	***trans*-3db**	8.7	−44.2	0.094	0.253	0.70
1e + 2c	***cis*-TSec**	***cis*-3ec**	12.0	−34.7	0.135	0.274	0.67
1e + 2c	***trans*-TSec**	***trans*-3ec**	17.0	−35.6	0.151	0.298	0.69
1c + 2c	***cis*-TScc**	***cis*-3cc**	9.1	−46.6	−0.050	0.284	0.67
1c +2c	***trans*-TScc**	***trans*-3cc**	9.9	−47.4	−0.072	0.233	0.73
1d + 2d	***cis*-TSdd**	***cis*-3dd**	11.1	−40.9	−0.035	0.255	0.70
1d + 2d	***trans*-TSdd**	***trans*-3dd**	12.2	−40.1	−0.061	0.243	0.71

[a] Computed at the B3LYP/6-31G*+ΔZPVE level of theory. [b] Computed at the B3LYP/6-31G* level of theory according to eq 2. [c] Computed at the B3LYP/6-31G* level according to eq 1.

the natural bond orbital (NBO) method.[25] According to eq 1, for a perfectly synchronous reaction, $Sy = 1$ since for any given bond index $\delta B_i = \delta B_{av}$. Similarly, according to eqs 2 and 3, early and late transition structures will be characterized by $\delta B_{av} < 0.5$ and $\delta B_{av} > 0.5$, respectively.

Donor−acceptor interactions were also computed using the NBO method. The energies associated with these two-electron interactions were computed by means of the second-order perturbation energy $\Delta E_{\phi\phi^*}^{(2)}$ according to the following equation:

$$\Delta E_{\phi\phi^*}^{(2)} = -n_\phi \frac{\langle \phi^* | \hat{F} | \phi \rangle^2}{\epsilon_{\phi^*} - \epsilon_\phi} \qquad (4)$$

where ϕ^* and ϕ are the non-Lewis and Lewis localized orbitals, $\hat{F}$ is the Fock operator, n_ϕ is the occupation of the ϕ localized orbital, and ϵ_{ϕ^*} and ϵ_ϕ are the respective energies.

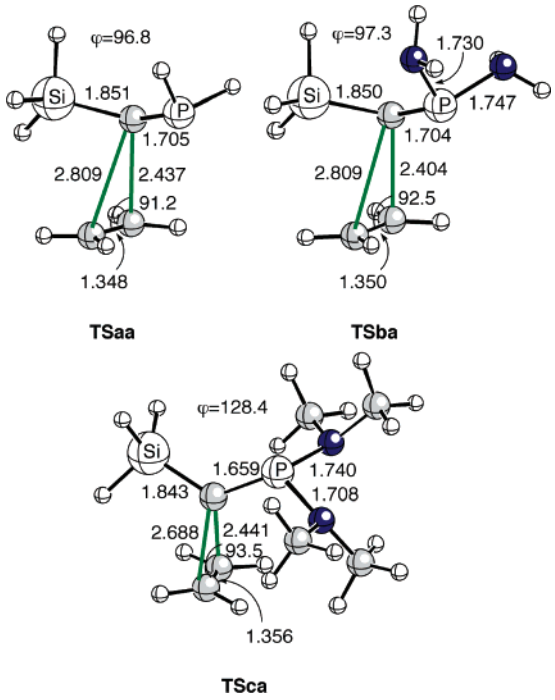

FIGURE 2. Fully optimized structures (B3LYP/6-31G* level) of transition structures **TSaa**, **TSba**, and **TSca** (Scheme 2). See Figure 1 caption for additional details.

All the stationary points were characterized by harmonic analysis.[26] Activation energies (ΔE_a) and reaction energies (ΔE_{rxn}) were computed at the B3LYP/6-31G* level including zero-point vibrational energy (ZPVE) corrections.

Within the ground-state parabola model,[16] the global hardnesses η were calculated[27] using the following expression:

$$\eta = I - A \approx \epsilon_{LUMO} - \epsilon_{HOMO} \qquad (5)$$

where I and A are the ionization potential and electron affinity, respectively, and ϵ_{LUMO} and ϵ_{HOMO} are the energies of the respective FMOs.[28] Similarly, chemical potentials μ were calculated

(25) (a) Reed, A. E.; Curtiss, L. A.; Weinhold, F. *Chem. Rev.* **1988**, *88*, 899. (b) Reed, A. E.; Weinstock, R. B.; Weinhold, F. *J. Chem. Phys.* **1985**, *83*, 735.
(26) McIver, J. W., Jr.; Komornicki, A. *J. Am. Chem. Soc.* **1972**, *94*, 2625.
(27) Parr, R. G.; von Szentpály, L.; Liu, S. *J. Am. Chem. Soc.* **1999**, *121*, 1922.

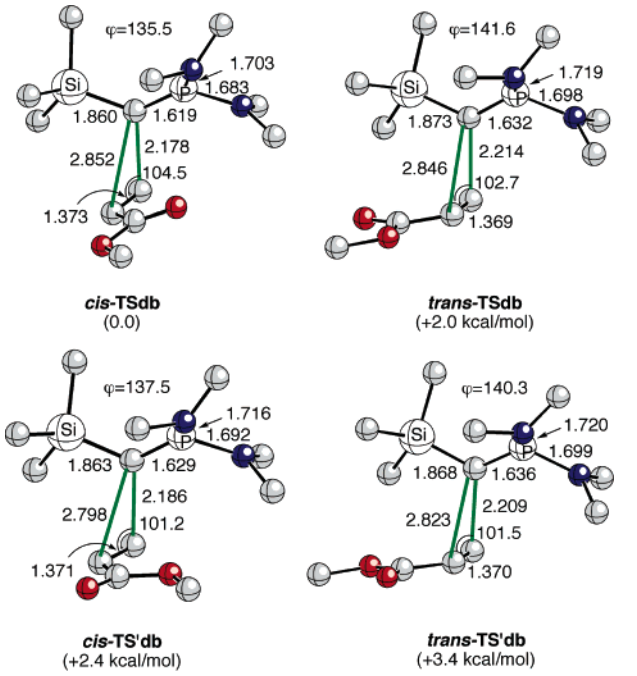

FIGURE 3. Fully optimized structures (B3LYP/6-31G* level) of transition structures ***cis*-TSdb** and ***trans*-TSdb** (Scheme 2). Transition structures ***cis*-TS′db** and ***trans*-TS′db** correspond to the respective conformers possessing s-trans-conformations about the methyl acrylate moiety. Numbers in parentheses are the relative energies. Hydrogen atoms have been omitted for clarity. Oxygen atoms are represented in red. See Figure 1 caption for additional details.

by means of the following equation:

$$\mu = -\frac{I + A}{2} \approx \frac{\epsilon_{HOMO} + \epsilon_{LUMO}}{2} \tag{6}$$

Within this framework, electrophilicities (ω) were calculated according to the proposal of Parr et al.[16]

$$\omega = \frac{\mu^2}{2\eta} \tag{7}$$

This expression for electrophilicity is similar to the description of power in classical electricity ($W = V^2/R$) and, according to Parr et al.,[16] ω can be considered as an electrophilic power since it encompasses the square of the propensity of the molecule to acquire additional electronic charge (term described by μ^2) and the resistance of the molecule to exchange electronic charge with the environment (term described by 2η). Finally, the maximum electronic charge ΔN_{max} that saturates electronically the molecule under consideration[16] is given by

$$\Delta N_{max} = -\frac{\mu}{\eta} \tag{8}$$

Both ω and ΔN_{max} magnitudes were computed by means of the approximate eqs 5 and 6. These magnitudes have proven to be useful to describe the reactivity in thermal cycloadditions.[29]

(28) Notice that in the valence-state parabola model, the hardness is given by $\eta = (I - A)/2$. See, for example: (a) von Szentpály, L. *Chem. Phys. Lett.* **1995**, *245*, 209. (b) von Szentpály, L. *J. Phys. Chem. A* **1998**, *102*, 10912.

(29) See, for example: Domingo, L. R.; Aurell, M. J.; Pérez, P.; Contreras, R. *Tetrahedron* **2002**, *58*, 4417.

Potential energy barriers of several reactions have been analyzed through the energy partition scheme implemented in the ADF[30] program using the OLYP[31] density functional and a triple-ζ plus polarization basis set. It has been recently shown that this functional provides results similar to B3LYP.[32]

For some reactions involving carbene **1e** (vide infra), the ONIOM[33] method was used. The system was divided into two layers. The first layer was treated at the B3LYP/6-31G* level of calculation, whereas for the second layer, the semiempirical AM1[34] method was used. This latter layer was formed by the peripheral methyl groups, the first layer including all the remaining atoms.

Results and Discussion

The structure and reactivity indices of (phosphino)(silyl)-carbenes **1a**−**e** were studied first. The main geometric features of these compounds are collected in Figure 1, and some of their computed properties are given in Table 1. According to our results, the minimum energy structures of singlet carbenes **1a**−**e** correspond to bent geometries, the Si−C−P bond angle being larger for compounds **1d,e**, in which the inductive effect of the bis(dialkylamino) groups is more pronounced. The calculated values of ca. 150° for this bond angle are in good agreement with the reported X-ray structure for a structurally related (phosphino)(silyl)carbene.[4d] The donating effect of the phosphino groups is clearly shown by the computed :C−P bond orders, which are very close to 2, whereas the respective :C−Si bond orders are close to 1 (Table 1). In addition, the computed natural charges are significantly larger than those obtained for singlet methylene and dichlorocarbene. All these results indicate that in these carbenes, the resonance form **II** contributes significantly to the actual structure, as is shown below.

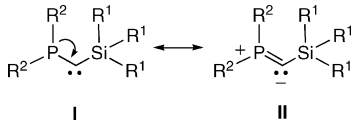

Molecular DFT-based parameters indicate that the stabilized carbenes **1b**−**e** are harder (i.e., more reluctant to acquire additional electronic density) than **1a**. This latter molecule is significantly harder than singlet methylene and dichlorocarbene (Table 1). The chemical potentials follow the opposite trend. In addition, the computed electrophilicities of stabilized carbenes **1b**−**e** are significantly lower than that of **1a**. As a reference, the computed electrophilicities of singlet methylene and dichlorocarbene are ca. 1.8 eV larger than that computed for **1a.** Finally, the ΔN_{max} values for carbenes **1b**−**e** are close to 0.5 e, whereas the corresponding value for **1a** is ca. 1 e. In contrast, both singlet methylene and dichlorocarbene can accept ca. 1.5 e, a value closer to the maximum of 2 e that one carbene can formally accept to complete its electronic octet.[35]

In summary, our calculations indicate that singlet (phosphino)-(silyl) carbenes **1b**−**e** are significantly more stable (harder) and

(30) (a) te Velde, G.; Bickelhaupt, F. M.; Baerends, E. J.; Fonseca, Guerra, C.; van Gisbergen, S. J. A.; Snijders, J. G.; Ziegler, T. *J. Comput. Chem.* **2001**, *22*, 931. (b) *ADF2005.01, SCM, Theoretical Chemistry*; Vrije Universiteit: Amsterdam, The Netherlands; http://www.scm.com.

(31) Handy, N. C.; Cohen, A. *J. Mol. Phys.* **2001**, *99*, 403.

(32) Baker, J.; Pulay, P. *J. Chem. Phys.* **2002**, *117*, 1441.

(33) Vreven, T.; Morokuma, K. *J. Comput. Chem.* **2000**, *21*, 1419.

(34) Dewar, M. J. S.; Zoebisch, E. G.; Healy, E. F.; Stewart, J. J. P. *J. Am. Chem. Soc*. **1985**, *107*, 3902.

(35) For a recent experimental and computational study on the basicity of this kind of carbenes, see: Martin, D.; Illa, O.; Baceiredo, A.; Bertrand, G.; Branchadell, V.; Ortuño, R. M. *J. Org. Chem.* **2005**, *70*, 5671.

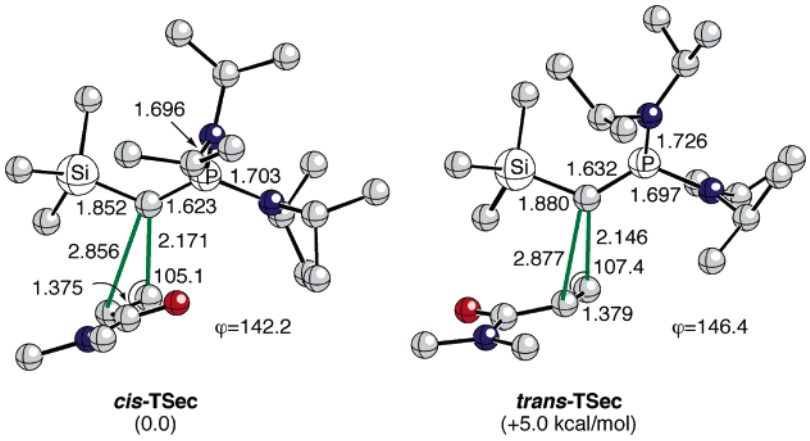

FIGURE 4. Fully optimized structures (B3LYP/6-31G* level) of transition structures ***cis*-TSec** and ***trans*-TSec** (Scheme 2). Numbers in parentheses are the relative energies. Hydrogen atoms have been omitted for clarity. Oxygen atoms are represented in red. See Figure 1 caption for additional details.

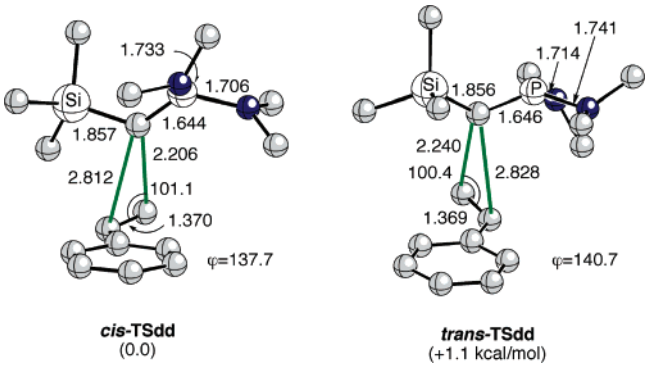

FIGURE 5. Fully optimized structures (B3LYP/6-31G* level) of transition structures ***cis*-TSdd** and ***trans*-TSdd** (Scheme 2). Numbers in parentheses are the relative energies. Hydrogen atoms have been omitted for clarity. See Figure 1 caption for additional details.

less electrophilic than ordinary carbenes.[36] This behavior is due to the donating effect of the phosphino moiety and to the positive inductive effect induced by the dialkylamino groups. This relatively low electrophilicity as well as the large charges of the reactive carbon atom, described by resonance form **II**, should result in nucleophilic transition structures in the corresponding [2 + 1] reaction with alkenes, as is shown in Scheme 3. As a consequence, the $r_{1'}$ distances and φ' angles should be larger than those observed for cyclopropanation reactions involving non-stabilized carbenes.[12]

The next step in our study was to analyze the main factors controlling the outcome of the reactions depicted in Scheme 2, some of them being very close or identical to experimentally studied transformations.[37] The activation and reaction energies as well as the charge-transfer values, synchronicities, and degrees of advancement of the corresponding transition structures are collected in Table 2.

We have found that the model reactions between ethylene **2a** and singlet carbenes **1a**−**c** take place via early transition structures, with δB_{av} values of ca. 0.2. The main geometric features of **TSaa**, **TSba**, and **TSca** are shown in Figure 2. According to our results, the reactions of the carbenes **1a**,**b** are very synchronous (see Table 2), and these carbenes behave as electrophiles, with negative charges for the carbene subunit of ca. −0.1 e at the correspondig transition structures. However, the interaction with **1c** is calculated to be more asynchronous. As expected for this electrophilic behavior, the computed φ values (Scheme 3) are of ca. 90°.

The analysis of the [2 + 1] cycloaddition between carbene **1d** and methyl acrylate **2b**[38] requires the computation of the transition structures corresponding to both the s-cis- and the s-trans-conformations of the ester **2b**. The four transition structures thus obtained are shown in Figure 3. As can be seen by the inspection of Figure 3, the s-cis-transition structures ***cis*-TSdb** and ***trans*-TSdb** are the most stable ones. This reaction leading to the formation of ***cis*-** and ***trans*-3db** is found to be much more asynchronous than the preceding transformations, the earliness of the corresponding transition structures being similar (Table 2). As expected from the lower electrophilicity of **1d** (vide supra) and the π deficient character of **2b**, the carbene moiety in both ***cis*-** and ***trans*-TSdb** has a globally positive charge of ca. 0.1 e (Table 2). Therefore, there is an electronic flux from the carbene to the α,β-unsaturated ester, thus resulting in a nucleophilic transition structure (Scheme 3). In agreement with this interpretation, the angle of the nucleophilic attack on the electrophilic β-carbon atom of the methyl acrylate subunit is larger than 90° (Figure 3). In addition, the $r_{1'}$ distances are larger than those found in **TSaa** and **TSba**. The low sychronicity of this reaction stems from the larger values of ca. 2.85 Å for these distances (Figure 3). Finally, the measured φ angles (Scheme 3) for these saddle points are of ca. 140°, also in agreement with nucleophilic transition structures. Our calculations also indicate that since ***cis*-TSdb** is ca. 2.0 kcal/mol more stable than ***trans*-TSdb** (Figure 3), only the corresponding cis-cycloadduct **3db** must be formed under kinetic

(36) These results are consistent with the singlet−triplet gaps computed for these kind of push−pull carbenes. See: (a) Schoeller, W. W.; Rozhenko, A. J. B.; Alijah, A. *J. Organomet. Chem.* **2001**, *617*−*618*, 435. (b) Canac, Y.; Conejero, S.; Donnadieu, B.; Schoeller, W. W.; Bertrand, G. *J. Am. Chem. Soc.* **2005**, *127*, 7312. For related studies on the stability of phosphorus-containing carbenes, see: (c) Fekete, A.; Nyulászi, L. *J. Organomet. Chem.* **2002**, *643*−*644*, 278.

(37) For pioneering experimental and computational studies on the reactivity of singlet carbenes in terms of selectivity (Isokinetic relationships), see: (a) Giese, B.; Meister, J. *Angew. Chem., Int. Ed. Engl.* **1978**, *17*, 595. (b) Schoeller, W. W. *Angew. Chem., Int. Ed. Engl.* **1981**, *20*, 698.

(38) The cyclopropanation reaction between carbene **1b** and **2b** resulted in strong stabilization of the corresponding cis-transition structures because of the formation of intramolecular hydrogen bonds between the amino groups of the model carbene and the carboxylate moiety of the α,β-unsaturated ester. Since it is not possible to reproduce this particular bonding in the experiments, we do no report these computational results here.

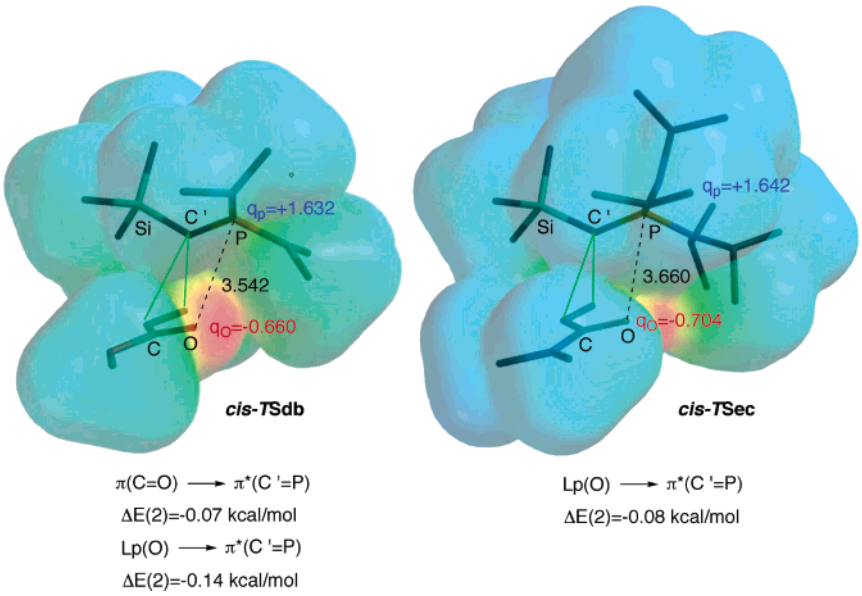

FIGURE 6. Electrostatic potentials projected onto electron densities (computed with an isovalue of 0.002 au) of fully optimized transition structures ***cis*-TSdb** and ***cis*-TSec**. Colors range from −74.2 kcal/mol (red) to +32.7 kcal/mol (blue). Distances between the P and O atoms are given in angstroms. Natural charges for these atoms (given in au) are denoted as q_P and q_O, respectively. The B3LYP/6-31G* values for the two-electron second-order perturbational energies between the indicated localized natural orbitals are also given. These values were calculated by means of eq 4.

TABLE 3. Partition of the Potential Energy Barriers×*bb* Δ*E* (in kcal/mol) for Several Reactions Depicted in Scheme 2, Involving Carbene 1c

reactants	TS	E_{prep}	E_{Pauli}	E_{elstat}	E_{orb}	$E_{C\rightarrow A}$	$E_{A\rightarrow C}$	E_{pol}	Δ*E*
1c + **2a**		10.1	65.0	−27.0	−31.2	−7.3	−12.3	−11.6	16.9
1c + **2b**	***cis*-TScb**	6.5	74.7	−33.6	−36.7	−15.0	−6.6	−15.1	10.9
1c + **2b**	***trans*-TScb**	8.3	64.6	−26.9	−32.4	−12.1	−7.4	−12.9	13.6
1c + **2c**	***cis*-TScc**	7.1	86.4	−39.7	−42.3	−17.7	−6.6	−18.0	11.5
1c + **2c**	***trans*-TScc**	9.1	63.4	−25.5	−31.4	−10.8	−8.1	−12.5	15.6
1c + **2d**	***Cis*-TScd**	8.6	69.2	−28.9	−34.5	−9.3	−11.6	−13.6	14.4
1c + **2d**	***trans*-TScd**	9.8	60.7	−24.4	−30.2	−7.1	−11.1	−12.0	15.9

×*bb*Computed at the OLYP/TZP level of calculation for geometries optimized at the B3LYP/6-31G* level. See eqs 9, 10, and text for additional details.

SCHEME 4. Experimentally Observed Reactivity of Carbene 1e toward Dimethyl Fumarate 2e and Maleate 2f

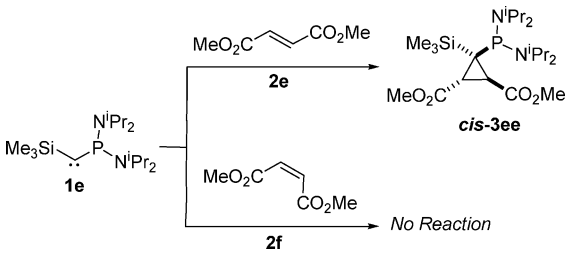

control, in excellent agreement with the experimental results,[6] although ***trans*-3db** is thermodynamically more stable than its cis-analogue (Table 2).

To study the behavior of *N*,*N*-dimethyl acrylamide **2c** in this [2 + 1] reaction, we started computing its interaction with carbene **1d**. Quite surprisingly, we found different stepwise reaction channels for the **1d** + **2c** → **3dc** reaction, aside from the concerted [2 + 1] thermal cycloaddition. Unfortunately, the additional reactions could not be observed experimentally since only carbene **1e** possessing more bulky isopropyl groups could be used in the cycloaddition experiments. In contrast, when we studied the interaction between carbene **1e** and **2c**, both reactions leading to either ***cis*-** and ***trans*-3ec** resulted in [2 + 1] concerted processes. The corresponding transition structures ***cis*-TSec** and ***trans*-TSec** are shown in Figure 4. Since in N,N-disubstituted acrylamides the s-cis-conformations are much more stable than the s-trans ones,[39] only the s-cis-transition structures shown in Figure 4 were investigated. Our results indicate that this reaction takes place via nucleophilic transition structures, whose main features are similar to those found for the reaction between **1d** and methyl acrylate **2b**. Interestingly, in spite of the bulkier character of the isopropyl groups of the carbene subunit with respect to the methyl groups present in the preceding case, the stereocontrol predicted by our computations in favor of ***cis*-3ec** via ***cis*-TSec** is higher than that predicted for the **1d** + **2b** → **3db** transformation (Figure 4), the corresponding activation energies also being higher (Table 2). In this case, the complete sterocontrol predicted by our calculation is in agreement with the exclusive formation of ***cis*-3ec** observed in the experimental studies.[6]

The reaction between carbene **1d** and styrene **2d** is somewhat different with respect to those previously studied involving electrophilic alkenes **2b**,**c**. The chief features of the corresponding transition structures ***cis*-TSdd** and ***trans*-TSdd** are reported in Figure 5. Although the geometries of these saddle points resemble those associated with nucleophilic transition states (i.e.,

(39) (a) Witanowski, M.; Stefaniak, L.; Dobrowolski, P.; Wojcik, J.; Webb, G. A. *Bull. Pol. Acad. Sci., Chem.* **1988**, *36*, 229. (b) Wojcik, J.; Witanowski, M.; Webb, G. A. *J. Mol. Struct.* **1978**, *49*, 249.

TABLE 4. Activation Energies ΔE_a (kcal/mol) for Reactions of Carbenes 1c,e with Dimethyl Fumarate 2e and Dimethyl Maleate 2f

***cis*-series**: X=SiR_3 (R=H, Me), Y=PR'_2 (R'=NMe_2, N*i*Pr_2)
***trans*-series**: X=PR'_2 (R'=NMe_2, N*i*Pr_2), Y=SiR_3 (R=H, Me)

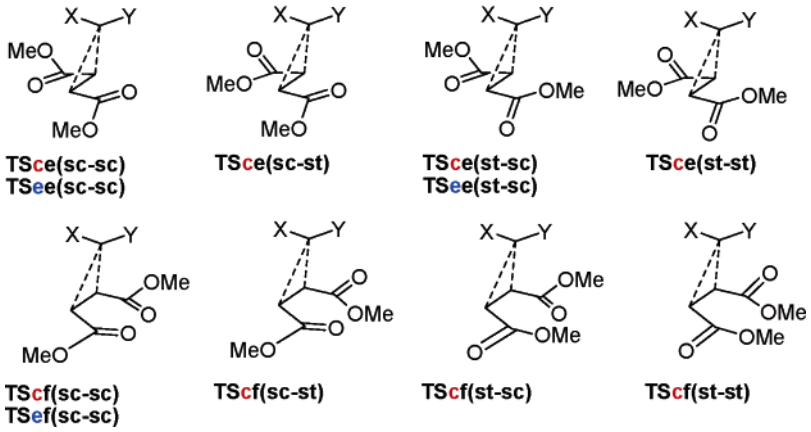

reactants	TS	ΔE_a	reactants	TS	ΔE_a
1c + 2e	*cis*-TSce(sc-sc)	5.4	**1c + 2f**	***cis*-TScf(sc-sc)**	6.4
1c + 2e	***cis*-TSce(sc-st)**	8.3	**1c + 2f**	***cis*-TScf(sc-st)**	9.3
1c + 2e	***cis*-TSce(st-sc)**	5.4	**1c + 2f**	***cis*-TScf(st-sc)**	7.7
1c + 2e	***cis*-TSce(st-st)**	8.1	**1c + 2f**	***cis*-TScf(st-st)**	12.7
1c + 2e	***trans*-TSce(sc-sc)**	8.1	**1c + 2f**	**trans-TScf(sc-sc)**	9.2
1c + 2e	***trans*-TSce(sc-st)**	8.9	**1c + 2f**	***trans*-TScf(sc-st)**	10.4
1c + 2e	***trans*-TSce(st-sc)**	11.6	**1c + 2f**	***trans*-TScf(st-sc)**	10.7
1c + 2e	***trans*-TSce(st-st)**	12.3	**1c + 2f**	***trans*-TScf(st-st)**	10.6
1e + 2e	***cis*-TSee(sc-sc)**	6.0 (8.6)[b]	**1e + 2f**	***cis*-TSef(sc-sc)**	9.3 (14.4)[b]
1e + 2e	***cis*-TSee(st-sc)**	6.6 (10.1)[b]			

[a] Computed at the B3LYP/6-31G*+ΔZPVE level of theory. [b] Computed at the ONIOM(B3LYP/6-31G*:AM1) + ΔZPVE level of calculation. In parentheses values computed at the B3LYP//ONIOM level of calculation.

low synchronicities and large φ values of ca. 140°), the electronic balance of the carbene moieties in both saddle points is lower than those computed for **TSaa** and **TSba**. This result indicates a weak electronic flux from the styrene subunit (Table 2). The activation energies predicted for this reaction indicate that the cycloadduct ***cis*-3dd** would be the major one, once again in good agreement with the experimental evidence.[6]

Up to now, we have reproduced correctly the complete *cis*-stereocontrol observed in these cyclopropanation reactions. The remaining question is the origin of this stereocontrol. In a previous paper,[6] it was suggested that this high stereoselectivity can be due to secondary orbital interactions (SOI)[40] between the LUMO of the carbene unit and the HOMO of the alkene. This LUMO can overlap with, for instance, the π(C═O) subunit of the HOMO associated with electrophilic alkenes like **2b** or **2c**. We have actively searched these SOI in our computational study. However, these stabilizing interactions resulted to be very small in magnitude. Thus, in ***cis*-TSdb**, the second-order energy associated with the donation from the π(C═O) localized natural orbital to the π^*(C′═P) acceptor is calculated to be ca. 0.1 kcal/mol only (Figure 6). Similarly, a donation between one lone pair of the sp^2-hybrydized oxygen atom of the acrylate and the π^*(C′═P) localized orbital results in a stabilization energy of ca. 0.2 kcal/mol. Similar effects were observed in ***cis*-TSec** (Figure 6). The large distances between the atoms involved (ca. 3.5−3.6 Å) make the overlap between the corresponding orbitals difficult. In addition, the stabilization induced by the P atom also results in a large energy of the LUMO of the carbene, thus augmenting the energy difference between donating and accepting orbitals, which results in a lower stabilization energy according to eq 4.

The alternative explanation for the observed complete cis-stereoselectivity is related to a combination of steric and electrostatic factors. It is clear that the trialkyl silyl groups introduce a strong steric congestion close to the substituent of the olefin, whereas the P atom sends the branching points of the bis(dialkylamino) groups and the steric hindrance thereof away from the stereogenic center of the alkene. This in turn creates a cavity in the cis-transition structure that can accommodate more easily the substituent of the olefin (see the 3-D eletron density maps in Figure 6). On the other hand, there is an attractive Coulombic interaction between the O and the P atoms, as is shown in Figure 6. The corresponding interatomic distance is enough to generate a stabilization energy of ca. 0.16 au. It is interesting to note that the negative charge in the oxygen atom of the *N*,*N*-dimethyl acrylamide subunit of ***cis*-TSec** generates a stabilization energy that is 3.4 kcal/mol larger than that found for ***cis*-TSdb**, in spite of the slightly larger interatomic distance (see Figure 6).

The electrostatic origin of the cis-stereoselectivity can also be related to the dipole moments of the reactant molecules. For example, the dipole moment of the carbene **1c** is 4.965 D and is parallel to the C−P axis ($C^{\delta(-)}-P^{\delta(+)}$). On the other hand, the computed dipole moments of methyl acrylate (1.498 D) and *N*,*N*-dimethylacrylamide (3.471 D) are parallel to the carbonyl

(40) (a) Woodward, R. B.; Hoffmann, R. *The Conservation of Orbital Symmetry*; Verlag Chemie: Weinheim, 1971. (b) Arrieta, A.; Cossío, F. P.; Lecea, B. *J. Org. Chem.* **2001**, *66*, 6178.

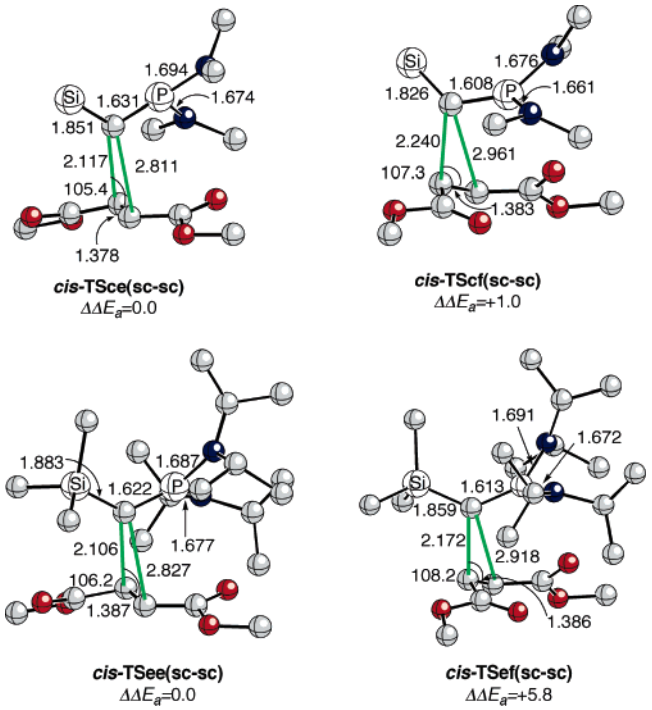

FIGURE 7. Fully optimized structures (B3LYP/6-31G* and ONIOM-(B3LYP/6-31G*:AM1) of transition structures ***cis*-TSce(sc-sc)**, ***cis*-TScf(sc-sc)**, ***cis*-TSee(sc-sc)**, and ***cis*-TSef(sc-sc)**. Hydrogen atoms have been omitted for clarity. See Figure 1 and 4 captions for additional details. For each pair of transition structures, the relative activation energies ($\Delta\Delta E_a$, in kcal/mol) are given. These values have been calculated at the B3LYP/6-31G*+ΔZPVE (**TSce** and **TScf**) and B3LYP/6-31G*//ONIOM(B3LYP/6-31G*:AM1)+ΔZPVE (**TSee** and **TSef**) levels.

group ($C^{\delta(+)}-O^{\delta(-)}$). So, the most favorable interaction between carbene and alkene dipoles is produced in the cis-transition states.

The potential energy barrier (ΔE) for a cycloaddition reaction between carbene **1c** and an alkene can be partitioned into several terms:

$$\Delta E = E_{\text{prep}} + E_{\text{Pauli}} + E_{\text{elstat}} + E_{\text{orb}} \qquad (9)$$

The preparation energy, E_{prep}, is the energy necessary to distort the reactant molecules from their equilibrium geometries to the geometries they have at the transition state. E_{Pauli} is the Pauli repulsion term associated to closed shell repulsions between carbene and alkene fragments at the transition state. E_{elstat} is the electrostatic interaction energy arising from the interaction between both fragments, each one having the electron density that it would have in the absence of the other fragment. The orbital interaction term, E_{orb}, arises when the electron densities of both fragments are allowed to relax and accounts for charge transfer and polarization. By selectively deleting fragment virtual orbitals, we have decomposed this term into three contributions:[41]

$$E_{\text{orb}} = E_{\text{C}\rightarrow\text{A}} + E_{\text{A}\rightarrow\text{C}} + E_{\text{pol}} \qquad (10)$$

The first term arises when only the first virtual orbital of the alkene is considered and can be related to charge transfer from the carbene to the alkene. $E_{\text{A}\rightarrow\text{C}}$ is the stabilization produced when only the first virtual orbital of the carbene is included and accounts for alkene to carbene charge transfer. Finally, E_{pol} is the additional stabilization gained when all virtual orbitals are included and can be associated to the polarization of both fragments.

The results obtained for the reaction between carbene **1c** and alkenes **2a**−**d** are presented in Table 3. The preparation energy term has its maximum value for the reaction with ethylene. For the other reactions, values associated to trans-transition states are larger than those corresponding to the cis-transition states. The magnitude of the Pauli repulsion term is closely related to the distance between carbene and alkene fragments at the transition states and presents the largest values for cis-transition states. On the contrary, the electrostatic interaction and the orbital interaction terms favor the cis-transition states. For the reactions of **2b** and **2c**, the difference between E_{elstat} corresponding cis- and trans-transition states is larger than the difference in E_{orb}, thus confirming the role played by electrostatic interaction in the cis-stereoselectivity.

The partition of the orbital interaction term shows two different situations. For ethylene and styrene, the stabilization associated to the alkene to carbene charge transfer is larger than that corresponding to the inverse transfer. On the other hand, for the reactions of methyl acrylate and *N*,*N*-dimethylacrylamide, the carbene to alkene transfer prevails. This result is consistent with the natural charges of carbene moieties presented in Table 2. $E_{\text{A}\rightarrow\text{C}}$ may be associated to a secondary orbital interaction. For the reactions of methyl acrylate and *N*,*N*-dimethylacrylamide, this term is slightly more stabilizing for the trans-transition states than for the cis ones, thus confirming that secondary orbital interactions do not play the main role in cis-stereocontrol.

One intriguing experimental result was obtained when carbene **1e** was allowed to react with dimethyl fumarate **2e** and dimethyl maleate **2f**.[6] Whereas in the former reaction the corresponding [2 + 1] cycloadduct ***cis*-3ce** was obtained with complete stereocontrol, the reaction between **1c** and the (*Z*)-congener of **2e** did not take place (Scheme 4). To understand the origins of this different behavior, we also studied the reactions of carbene **1c** with dimethyl fumarate **2e** and dimethyl maleate **2f**. The reaction with **2e** leads to the formation of only one product, but different transitions states are possible. First, there are two different approaches for the initial attack of the carbene, which will be named cis and trans by analogy with the reaction with methyl acrylate. Moreover, s-cis/s-trans-conformations of the two ester groups must be considered. This leads to a total of eight possible transition state structures. The computed activation energies are shown in Table 4, in which sc/st descriptors indicate the conformation of the carboxylate moiety. The first label corresponds to the ester group vicinal to the alkene carbon atom involved in the formation of the first bond, while the second one corresponds to the other ester group. In the most stable conformer of isolated **2e**, both ester groups are s-cis, and s-cis/s-trans- and s-trans/s-trans-conformers are 0.8 and 1.5 kcal/mol higher in energy, respectively.

The reaction with **2f** may lead to two different products, cis and trans. For each one, we located four different transition state structures, differing from each other on the s-cis/s-trans-conformation of both ester groups. The corresponding activation energies have been included in Table 4. For isolated **2f**, the most stable conformer is s-cis/s-trans, while the s-trans/s-trans

(41) For previous examples describing this approach, see: (a) González-Blanco, O.; Branchadell, V.; Greé, R. *Chem.—Eur. J.* **1999**, *5*, 1722. (b) González-Blanco, O.; Branchadell, V. *Organometallics* **1997**, *16*, 5556.

one is 1.1 kcal/mol higher in energy and the s-cis/s-cis is not an energy minimum.

In the reaction between **1c** and dimethyl fumarate **2e**, the s-cis-conformation of the most remote ester group is clearly favored, as was the case for the reaction of methyl acrylate. For the ester group vicinal to the alkene carbon atom involved in the shortest bond being formed, both s-cis- and s-trans-conformations lead to nearly the same activation energy (5.42 and 5.39 kcal/mol for ***cis*-TSce(sc-sc)** and ***cis*-TSce(st-sc)**, respectively). The activation energy increases 0.4 kcal/mol with respect to the value corresponding to the reaction of methyl acrylate (Table 2).

In the case of the reaction between dimethyl maleate **2f** and carbene **1c**, the most favorable transition structure is the one in which both ester groups present a s-cis-conformation (***cis*-TScf-(sc-sc)**, see Table 4). The computed activation energy, 6.4 kcal/mol, is only 1 kcal/mol larger than the value corresponding to the reaction with **2e**. If we assume that the ratio of rate constants for the reactions of carbene **1c** with **2e** and **2f** is determined only by the difference in activation energies, the *k*(**2e**)/*k*(**2f**) ratio at 25 °C is 5.4. As we have already mentioned, the reaction between a phosphino(silyl)carbene and **2e** has been reported, but no reaction has been observed with **2f**. A rate constant ratio of 5.4 does not seem to be large enough to explain the different experimental behavior of both diesters. This is probably due to the model carbene **1c** used in the calculations since it lacks the steric requirements of the carbene **1e** used in experiments. We therefore studied the reactions of **2e** and **2f** with **1e**. Because of the size of the system, we used the ONIOM approach. In both the fumarate and the maleate series, the most stable transition structures were those possessing the ester groups in a s-cis-conformation (***cis*-TSee(sc-sc)** and ***cis*-TSef(sc-sc)**, see Figure 7 and Table 4). In both cases, we performed single-point calculations at the B3LYP/6-31G* level of calculation using the geometries optimized with the ONIOM method.

The difference between activation energies for the reactions of **2e** and **2f** are 3.3 kcal/mol (ONIOM reasults) and 5.8 kcal/mol (B3LYP results). These values are much larger than the difference computed for the reactions with carbene **1c**. For the reactions with **1e**, the ratio of rate constants *k*(**2e**)/*k*(**2f**) at 25 °C becomes 263 (ONIOM) and 1420 (B3LYP). These values are much more consistent with the lack of reactivity of dimethyl maleate in front of **1e** and suggest that this anomalous behavior is due to the steric congestion generated by the bulky trimethylsilyl and isopropylamino groups (Figure 7).

Conclusion

From the results reported in this paper, the following general conclusions can be drawn: (i) The [2 + 1] thermal cycloaddition between singlet (phosphino)(silyl) carbenes and alkenes takes place via concerted mechanisms. (ii) The nature of the transition structures in general reflects the nucleophilic character of these particularly stable singlet carbenes. (iii) The experimentally observed cis-stereoselectivity for these reactions can be rationalized in terms of a combination of steric and, specially, electrostatic effects rather than as a consequence of secondary orbital interactions. (iv) The chemistry of this kind of carbenes is very sensitive to substituent effects. Therefore, a correct description of these [2 + 1] cycloadditions usually requires the inclusion in the calculations of the same groups used in the experimental studies.

Acknowledgment. We thank the Ministerio de Educación y Ciencia of Spain (Projects CTQ2004-06816/BQU and CTQ2004-01067/BQU), the Gobierno Vasco-Eusko Jaurlaritza (Grant 9/UPV 00170.215-13548/2001) and the Generalitat de Catalunya (Grants PICS2005-10 and SGR2005-103) for financial support.

Supporting Information Available: Cartesian coordinates and energies (including zero-point vibrational energies) of all the reactants, intermediates, products, and transition structures discussed in this paper. This material is available free of charge via the Internet at http://pubs.acs.org.

JO061662V